Research Square

Preprints are preliminary reports that have not undergone peer review.
They should not be considered conclusive, used to inform clinical practice,
or referenced by the media as validated information.

THERMAL SAFETY OF SIMULATED ENDOSCOPIC LASER LITHOTRIPSY: AN IN VIVO PORCINE STUDY

Vigen A. Malkhasyan[1]
Botkin City Clinical Hospital
Vineet Gauhar
Ng Teng Fong General Hospital
Bhaskar K. Somani
University Hospital Southampton NHS Foundation Trust
Sergey O. Sukhikh[1]
docsukhikh@gmail.com

Botkin City Clinical Hospital
Igor O. Gritskov[1]
Russian University of Medicine
Leonid V. Reshetov[1]
Botkin City Clinical Hospital
Ali Talyshinskii
Genome Clinic
Nariman K. Gadzhiev
Saint Petersburg State University Hospital
Arman Tsaturyan
Yerevan State Medical University
Dmitry Yu. Pushkar[1]
Russian University of Medicine

Research Article

Keywords: Urolithiasis, retrograde intrarenal surgery, holmium:YAG laser, thulium fiber laser, intrarenal temperature, irrigation rate, CEM43, thermal safety

Posted Date: November 16th, 2026

DOI: https://doi.org/10.21203/rs.3.rs-11236664/v1

License: This work is licensed under a Creative Commons Attribution 4.0 International License.
Read Full License

Additional Declarations: No competing interests reported.

THERMAL SAFETY OF SIMULATED ENDOSCOPIC LASER LITHOTRIPSY: AN IN VIVO PORCINE STUDY

Vigen A. Malkhasyan[1,2], Vineet Gauhar[3,4], Bhaskar K. Somani[5], Sergey O. Sukhikh[1], Igor O. Gritskov[1,2], Leonid V. Reshetov[1], Ali Talyshinskii[6], Nariman K. Gadzhiev[7], Arman Tsaturyan[8,9], Dmitry Yu. Pushkar[1,2]

[1] Botkin City Clinical Hospital, Moscow, Russia

[2] Russian University of Medicine, Moscow, Russia

[3] Department of Urology, Ng Teng Fong General Hospital, Singapore, Singapore

[4] Asian Institute of Nephrourology, AINU, Hyderabad, India

[5] Department of Urology, University Hospital Southampton NHS Foundation Trust, Southampton, United Kingdom

[6] Department of Urology and Andrology, Genome Clinic, Astana, Kazakhstan

[7] Saint Petersburg State University Hospital, Saint Petersburg, Russia

[8] Department of Urology, Yerevan State Medical University, Yerevan, Armenia

[9] Department of Urology, Erebouni Medical Center, Yerevan, Armenia

Corresponding author: Sergey Sukhikh, PhD. Department of Urology, Botkin City Clinical Hospital. 2nd Botkinsky Proezd, Moscow 125284, Russia. Email: docsukhikh@gmail.com

Abstract

Background: Laser activation during retrograde intrarenal surgery may increase intrarenal temperature and cause thermal injury. In vivo data linking critical temperature thresholds to morphological changes remain limited. Objective: To compare temperature dynamics in the

renal collecting system and parenchyma during simulated lithotripsy with Ho:YAG and TFL in an in vivo porcine model.

Methods: Ten pigs were included. Temperature was recorded simultaneously in the collecting system and renal parenchyma using thermocouples. Ho:YAG and TFL were evaluated at 25 and 35 W with irrigation rates of 15 and 20 mL/min during 120 seconds of continuous activation without a stone or stone phantom. Intrarenal and parenchymal temperatures, time to 43 and 56 °C, critical thermal dose (CEM43 >120), and histopathological changes were assessed.

Results: Median intrarenal temperature remained below 43 °C only at 25 W and 20 mL/min for both lasers. Median temperature did not reach 56 °C, while peaks above 56 °C occurred only with Ho:YAG at 35 W and 15 mL/min. Increasing power from 25 to 35 W increased median intrarenal temperature by approximately 9–10 °C, whereas increasing irrigation from 15 to 20 mL/min reduced it by approximately 5 °C. Differences between lasers were comparatively modest (1.88–2.25 °C). CEM43 >120 occurred at 35 W and 15 mL/min for both lasers and at 35 W and 20 mL/min for Ho:YAG. Parenchymal temperature remained below 43 °C in all experiments. Histologically confirmed injury occurred exclusively at 35 W and 15 mL/min and was comparable between lasers; maximum injury depth was 410.4 µm for TFL and 590.3 µm for Ho:YAG.

Conclusions: Laser power, irrigation rate, and continuous activation time had a greater influence on thermal risk than laser type. The 35 W/15 mL/min condition showed the highest risk, whereas 25 W with 15–20 mL/min provided a more favorable safety profile in this model. Clinical trial number: not applicable.

Keywords: Urolithiasis, retrograde intrarenal surgery, holmium:YAG laser, thulium fiber laser, intrarenal temperature, irrigation rate, CEM43, thermal safety.

Background. Urolithiasis remains one of the most prevalent urinary tract disorders [1]. Laser lithotripsy represents the cornerstone of retrograde intrarenal surgery (RIRS). For many years, the holmium:YAG (Ho:YAG) laser has been regarded as the gold standard due to its capacity to fragment stones of virtually any chemical composition [2]. In recent years, the thulium fiber laser (TFL) has gained increasing clinical adoption, offering distinct technical characteristics, including the capability to operate at higher pulse frequencies and a different emission wavelength [3]. These features have generated interest in potential differences between the two laser systems, particularly in the context of thermal safety. Since laser activation is inherently associated with heat generation, preventing thermal injury to surrounding tissues remains an important consideration in contemporary endourology.

Exposure of biological tissues to 43 °C for 120 minutes has been associated with irreversible cellular injury, whereas exposure to 56 °C may result in irreversible damage within approximately one second [4]. Current studies demonstrate that maintaining an adequate irrigation rate and limiting laser power settings can reduce intrarenal temperature and, consequently, the risk of thermal tissue injury. However, most investigations addressing this issue have been conducted in vitro or using simplified bench-top models that do not account for tissue perfusion, heat dissipation, and the anatomical configuration of the renal collecting system. Consequently, temperature profiles obtained in vivo may differ substantially from those observed in laboratory simulations. Moreover, most published studies have focused solely on intrarenal temperature measurements within the collecting system, without assessing parenchymal temperature or corresponding histological alterations.

Another important challenge involves the clinical interpretation of transient temperature peaks. Emerging evidence suggests that not only the peak temperature but also the duration

of exposure determines the likelihood of tissue injury, a concept reflected in cumulative equivalent minutes at 43 °C (CEM43). Nevertheless, the application of this thermal dose model in endourological research remains limited.

A recent review by Tonyali et al. reported that the threshold thermal dose (CEM43 >120) may be exceeded even under standard laser settings, particularly during prolonged continuous activation and restricted irrigation [5]. The authors emphasized the role of laser power, irrigation parameters, and outflow conditions in shaping the intrarenal thermal profile, highlighting the need to balance temperature reduction through increased irrigation with the potential risk of elevated intrarenal pressure. Despite the clinical relevance of these findings, in vivo data evaluating histological changes induced by elevated intrarenal temperatures remain scarce. To date, comprehensive studies analyzing the relationship between intrarenal temperature, parenchymal temperature, and corresponding histopathological tissue alterations are lacking, underscoring the need for further investigation in this area.

Accordingly, the present study aimed to compare, in vivo, intrarenal temperature dynamics within the collecting system and parenchymal temperature changes during simulated laser lithotripsy using Ho:YAG and TFL systems at different laser power settings and irrigation rates, and to assess the associated histopathological effects on the renal parenchyma.

Methods. The study was conducted in a veterinary laboratory at the “Praxi Medica” Medical Practice Training Center (Sechenov University). Ten clinically healthy one-year-old female pigs (20 kidneys) were included in the study. The animals were purchased from Mashkino Livestock Complex LLC (Kolomna, Moscow Region, Russia) by the vivarium of Sechenov University and provided for the study at the Praxi Medica Medical Practice Training Center. This experimental model was selected due to the high anatomical and functional similarity

of the porcine urinary system to that of humans, making it suitable for evaluating thermal effects during laser lithotripsy.

All animals were confirmed to be clinically healthy based on preoperative veterinary examination. The animals were delivered to the laboratory on the day of the procedure and euthanized upon completion of the experimental protocol.

Surgical procedure and experimental setup.

Animals weighed 30–35 kg, and drug doses were individually adjusted according to body weight. Intramuscular diphenhydramine was administered 15 min before induction. Anesthesia was induced with intramuscular tiletamine–zolazepam (Zoletil) and xylazine. Following tracheal intubation with a cuffed tube, anesthesia was maintained with sevoflurane (reported vaporizer setting, 5%) and intravenous boluses of tiletamine–zolazepam. Intravenous rocuronium was administered every 20–25 min for neuromuscular blockade. Mechanical ventilation was provided at a tidal volume of 10 mL/kg and a respiratory rate of 12 breaths/min, with an inspired oxygen fraction of 0.30–0.35. Monitoring included electrocardiography, heart rate, pulse oximetry, and body temperature. Intravenous fluids comprised 0.9% sodium chloride and 5% glucose, administered as required at approximately 6 mL/kg/h. The animals were positioned supine on the operating table. Following a standard midline laparotomy, bilateral exposure of the kidneys and ureters was performed with preservation of the renal vascular supply and surrounding structures. In cases of bladder distension, the bladder was punctured and its contents were aspirated.

To access the renal collecting system, the distal third of the ureter was transected, and the ureteral lumen was dilated using a plastic bougie up to 10 Fr. An intraluminal thermocouple was advanced through the ureter into the renal collecting system to record intrarenal temperature. A 10/12 Fr ureteral access sheath was inserted over a hydrophilic guidewire,

with its distal tip positioned at the level of the ureteropelvic junction. A 7.5 Fr ureterorenoscope (HugeMed, China) was introduced through the access sheath. A 200 µm laser fiber was inserted through the working channel. The laser fiber tip and intrarenal thermocouple were positioned within the renal pelvis at a distance of 10 mm from each other. Laser activation was performed without a stone or stone phantom because reproducible placement and stable positioning of a stone or stone phantom at a standardized location within the porcine renal collecting system could not be technically ensured. Consequently, the experimental model was designed to assess continuous laser-induced heating under standardized non-contact conditions rather than to reproduce a specific lithotripsy technique. Direct contact between the laser fiber and the urothelium or renal tissue was avoided throughout laser activation. To minimize respiratory movement of the kidney and maintain stable positioning of the ureteroscope, laser fiber, and thermocouples, each 120-second laser activation was performed during controlled apnea induced by temporary suspension of mechanical ventilation. The positions of the ureteroscope, laser fiber, and thermocouples were maintained as stable as technically feasible throughout the activation period. A second thermocouple was placed in the renal parenchyma. Following needle puncture, the thermocouple was advanced into the created parenchymal tract to a depth of 5 mm without additional fixation. The positions of the intrarenal and parenchymal thermocouples and the laser fiber are shown in Figures 1 and 2.

Laser systems and irrigation protocol.

Two laser systems were used: a holmium:YAG (Ho:YAG) laser and a thulium fiber laser (TFL). The Ho:YAG laser system Litho (Quanta System, Italy), with a wavelength of 2.1 µm, operated in pulsed mode using a 200 µm laser fiber. The TFL system Urolase+ PREMIUM (VPG Photonics, USA), with a wavelength of 1.94 µm, was also used with a 200 µm laser fiber.

For each laser system, two power settings were applied: 25 W (Ho:YAG: 2.5 J × 10 Hz; TFL: 0.5 J × 50 Hz) and 35 W (Ho:YAG: 2.5 J × 14 Hz; TFL: 0.7 J × 50 Hz). Laser activation was continuous for 120 seconds.

Irrigation was performed passively using gravitational flow with sterile 0.9% NaCl solution maintained at room temperature (23 °C). The irrigation rate was regulated by adjusting the height of the irrigation bag relative to the kidney. For each laser power setting, two irrigation rates were used: 15 mL/min, with the irrigation bag positioned 82 cm above the kidney, and 20 mL/min, with the irrigation bag positioned 124 cm above the kidney. Before each experiment, the irrigation system was pre-flushed for one minute to verify that the actual irrigation rate corresponded to the target value.

Temperature was recorded every second in real time using Type K, Class 1 thermocouples (NiCr–NiAl) with a sensitivity of 50–60 μV/°C. The manufacturer-specified accuracy of the thermocouples was ±1.5 °C or ±0.4%.

Experimental series and temperature assessment.

Each kidney was considered an experimental unit. For each laser system, four primary experimental conditions were evaluated using different combinations of laser power and irrigation rate:

1. 25 W × 15 mL/min;
2. 25 W × 20 mL/min;
3. 35 W × 15 mL/min;
4. 35 W × 20 mL/min.

Each experimental kidney was assigned to a single combination of laser type, laser power, and irrigation rate and underwent only one 120-second laser activation. No kidney was

reused across experimental conditions. For each experimental condition, two independent experimental runs were performed, each in a separate kidney. Thus, 16 kidneys were used across the eight primary experimental conditions. Two additional kidneys served as untreated controls without laser activation, providing baseline histological reference specimens. The remaining two kidneys were used in supplementary experiments to verify temperature measurements under the conditions that demonstrated the greatest variability in peak temperature.

Threshold temperatures of 43 and 56 °C were used as reference points. These values were based on the cellular thermal injury model described by Sapareto and Dewey [4], according to which the degree of biological damage depends not only on the temperature achieved but also on the duration of exposure. The rate of thermal injury increases exponentially with increasing temperature. An exposure of 120 minutes at 43 °C corresponds to a thermal dose of 120 cumulative equivalent minutes at 43 °C. At 50 °C, an equivalent thermal dose is reached in less than one minute, whereas at 56 °C it may be reached within approximately one second.

Thermal dose was expressed as cumulative equivalent minutes at 43 °C (CEM43) and calculated using the following equation:

$$t_{43} = \sum_i R^{(43-T_i)} \Delta t_i$$

where t_{43} is the equivalent exposure time at 43 °C, T_i is the local temperature at time point i, Δt_i is the time interval expressed in minutes, and R is the temperature coefficient equal to 0.5 for $T_i \geq 43$ °C and 0.25 for $T_i < 43$ °C.

The assessed temperature-related outcomes included intrarenal and parenchymal temperatures, time to reach the threshold temperatures of 43 and 56 °C, and exceedance of the critical thermal dose defined as CEM43 >120.

Histopathological assessment.

Following completion of all experimental series, bilateral nephrectomy was performed. The excised kidneys were fixed in 10% neutral buffered formalin (pH 7.2–7.4) for 24 hours at room temperature. After fixation, representative tissue samples of the renal cortex and medulla were obtained, including areas adjacent to the presumed zone of thermal exposure.

The samples were placed in tissue cassettes and subjected to automated tissue processing through graded alcohols, xylene, and paraffin. The specimens were subsequently embedded in paraffin, and 4–5 μm sections were prepared using a rotary microtome. The sections were deparaffinized and stained with hematoxylin and eosin to assess tissue architecture and cellular changes. After staining, the slides were mounted with coverslips and examined by light microscopy using a Zeiss Primo Star microscope (Zeiss, Germany). Histopathological evaluation was performed by a pathologist blinded to the experimental group allocation. Morphometric evaluation included assessment of the depth and extent of thermally altered tissue zones, severity of interstitial edema, vascular reactions, presence of coagulative necrosis, and tubular epithelial damage. The histopathological findings were correlated with the recorded temperature profiles to evaluate the relationship between the degree of thermal injury and local hyperthermia.

Statistical analysis.

Temperature data were analyzed descriptively using IBM SPSS Statistics version 26.0. For each primary experimental condition, temperature measurements were obtained from two kidneys and recorded once per second during 120 seconds of continuous laser activation. At each time point, the values obtained from the two kidneys were averaged, and the standard error of the mean (SEM) was calculated to illustrate variability between the two measurements, generating a 120-point mean temperature profile for each condition.

Because serial temperature measurements obtained within the same kidney were temporally correlated and only two kidneys were evaluated per primary experimental condition, individual time points were not treated as independent experimental units, and no formal hypothesis testing was performed. Temperature profiles were summarized descriptively using median values with interquartile ranges [Q1; Q3], peak temperatures, and absolute differences between experimental conditions. Additional outcomes included the time required to reach the temperature thresholds of 43 and 56 °C and the time required to exceed the critical thermal dose of CEM43 >120.

Temperature curves are presented as pointwise mean values. SEM was calculated to describe variability between the two measurements and is reported for descriptive purposes only; given the limited number of kidneys per condition, it should not be interpreted as an estimate of population-level precision. Given the limited number of kidneys per condition, SEM values are provided for descriptive purposes only and should not be interpreted as estimates of population-level precision. Histopathological findings were analyzed qualitatively and compared descriptively with the corresponding temperature profiles and thermal dose calculations.

Use of generative artificial intelligence

During the preparation of this manuscript, the authors used ChatGPT (OpenAI) for English-language editing and stylistic refinement. Generative artificial intelligence was not used to generate or analyse experimental data or perform statistical calculations. The authors reviewed the final text and take full responsibility for its content.

Results.

Intrarenal and parenchymal temperatures.

During Ho:YAG laser activation at 25 W, median intrarenal temperature was 45.25 °C at an irrigation rate of 15 mL/min and 41.50 °C at 20 mL/min. At 35 W, median intrarenal temperature was 55.27 °C at 15 mL/min and 50.25 °C at 20 mL/min (Table 1). Peak intrarenal temperature exceeded 56 °C only during Ho:YAG activation at 35 W and 15 mL/min, reaching 56.13 °C (Table 2, Figure 3).

During TFL activation at 25 W, median intrarenal temperature was 43.37 °C at an irrigation rate of 15 mL/min and 39.25 °C at 20 mL/min. At 35 W, median intrarenal temperature was 53.12 °C at 15 mL/min and 48.00 °C at 20 mL/min (Table 1). Peak intrarenal temperature did not exceed 56 °C under any TFL setting (Table 2, Figure 3). The maximum standard error across all temperature measurements did not exceed 1.125 °C.

Thus, median intrarenal temperature remained below 43 °C only at 25 W and an irrigation rate of 20 mL/min for both laser systems.

Neither median nor peak parenchymal temperature exceeded 43 °C in any experiment. The highest median parenchymal temperature was 39.33 °C during Ho:YAG activation at 35 W and 15 mL/min. Under the same conditions, the highest peak parenchymal temperature was 40.38 °C (Tables 1 and 2, Figure 4).

Effect of laser power on intrarenal temperature.

At an irrigation rate of 15 mL/min, increasing Ho laser power from 25 to 35 W increased median intrarenal temperature by 10.02 °C, from 45.25 to 55.27 °C. Under the same irrigation conditions, increasing TFL power from 25 to 35 W increased median intrarenal temperature by 9.75 °C, from 43.37 to 53.12 °C. At an irrigation rate of 20 mL/min, increasing laser power from 25 to 35 W increased median intrarenal temperature by 8.75 °C for both laser systems: from 41.50 to 50.25 °C for Ho and from 39.25 to 48.00 °C for TFL (Figures 5 and 6).

Effect of irrigation rate on intrarenal temperature.

At a laser power of 25 W, increasing the irrigation rate from 15 to 20 mL/min decreased median intrarenal temperature by 3.75 °C for Ho:YAG, from 45.25 to 41.50 °C, and by 4.12 °C for TFL, from 43.37 to 39.25 °C. At a laser power of 35 W, increasing the irrigation rate from 15 to 20 mL/min decreased median intrarenal temperature by 5.02 °C for Ho:YAG, from 55.27 to 50.25 °C, and by 5.12 °C for TFL, from 53.12 to 48.00 °C (Figures 5 and 6).

Effect of laser type on intrarenal temperature.

At 25 W and an irrigation rate of 15 mL/min, median intrarenal temperature was 45.25 °C with Ho:YAG and 43.37 °C with TFL, corresponding to an absolute difference of 1.88 °C (Figure 7). At the same laser power and an irrigation rate of 20 mL/min, median intrarenal temperature was 41.50 °C with Ho:YAG and 39.25 °C with TFL, corresponding to a difference of 2.25 °C (Figure 8).

At 35 W and an irrigation rate of 15 mL/min, median intrarenal temperature was 55.27 °C with Ho:YAG and 53.12 °C with TFL, corresponding to a difference of 2.15 °C (Figure 9). At the same laser power and an irrigation rate of 20 mL/min, median intrarenal temperature was

50.25 °C with Ho:YAG and 48.00 °C with TFL, corresponding to a difference of 2.25 °C (Figure 10).

Time to reach the threshold temperatures and critical thermal dose.

During Ho:YAG activation at 25 W and an irrigation rate of 15 mL/min, the 43 °C threshold was reached in 19 seconds, whereas at 20 mL/min this threshold was not reached. At 35 W, the 43 °C threshold was reached in 5 seconds at an irrigation rate of 15 mL/min and in 13 seconds at 20 mL/min. The 56 °C threshold was reached only during Ho:YAG activation at 35 W and 15 mL/min, after 60 seconds of continuous laser activation.

During TFL activation at 25 W and an irrigation rate of 15 mL/min, the 43 °C threshold was reached in 26 seconds, whereas at 20 mL/min it was not reached. At 35 W, the 43 °C threshold was reached in 9 seconds at an irrigation rate of 15 mL/min and in 16 seconds at 20 mL/min. The 56 °C threshold was not reached under any TFL setting (Table 3).

Exceedance of the critical thermal dose threshold (CEM43 >120) was observed for both laser systems at 35 W and 15 mL/min and during Ho:YAG activation at 35 W and 20 mL/min. During Ho:YAG activation at 35 W and 15 mL/min, CEM43 >120 was reached in 13 seconds; at 35 W and 20 mL/min, this threshold was reached in 33 seconds. During TFL activation at 35 W and 15 mL/min, CEM43 >120 was reached in 23 seconds.

Histopathological findings.

Histopathological analysis confirmed an association between temperature elevation and structural renal tissue injury (Table 4). Reproducible morphological alterations were observed only during laser activation at 35 W and an irrigation rate of 15 mL/min.

During TFL activation at 35 W and 15 mL/min, diffuse renal tissue injury was observed in both specimens, with injury depths of 332.4 and 410.4 μm, respectively (Figure 11). Macroscopically, localized areas of thermal injury were identified within the renal pelvis.

During Ho:YAG activation under identical conditions, tissue injury was comparable in distribution but more pronounced in depth. Diffuse coagulative changes involving the urothelial and suburothelial layers were observed, with extension into the superficial renal parenchyma in some areas. The reported injury depth ranged from 485.1 to 590.3 μm (Figures 12 and 13).

No reproducible histopathological alterations were identified in the examined tissue sections under the other combinations of laser power and irrigation rate. All findings were compared with control histological specimens obtained from kidneys not subjected to laser activation (Figure 14).

Discussion. To date, a limited number of studies have been published that directly or indirectly assessed intrarenal temperature dynamics during retrograde intrarenal surgery. The vast majority of these investigations were conducted using bench-top, in vitro, or ex vivo models, or represent descriptive clinical case series in which temperature parameters were recorded without standardized assessment of tissue-level thermal injury. In addition, approximately six review and systematic review articles have summarized available data on intrarenal temperature and thermal risk factors during endourological procedures.

Despite the substantial body of experimental evidence, in vivo animal data remain relatively limited. Most available studies have focused primarily on intrarenal fluid temperature, whereas simultaneous assessment of renal parenchymal temperature has been performed only in a minority of investigations. Direct comparative analyses of temperature profiles between Ho:YAG and TFL systems also remain scarce. Histological verification of thermal

injury represents another important gap in the literature. Only a limited number of experimental studies have included morphological assessment of laser-induced thermal effects, and these have mainly focused on ureteral tissue rather than on the renal collecting system or renal parenchyma.

In the present study, we employed an in vivo model that accounts for tissue perfusion and physiological heat dissipation to directly compare temperature profiles of Ho:YAG and TFL systems. The analysis included assessment of intrarenal temperature dynamics, time to reach peak temperature thresholds, exceedance of the critical thermal dose (CEM43 >120), and histopathological evaluation of renal tissue. Such a comprehensive design distinguishes this study from previously published investigations in this field.

In recent years, the thermal impact of laser lithotripsy on renal tissue has been actively investigated. The majority of recent studies indicate that the risk of thermal injury is multifactorial and determined by laser power, irrigation rate, duration of continuous laser activation, and the volume of irrigation fluid within the renal collecting system. In our experiment, a direct relationship between intrarenal temperature and laser power was demonstrated, as well as an inverse relationship with irrigation rate. These findings support the concept that thermal safety depends on maintaining an optimal balance between laser power and irrigation rate, along with limiting the duration of continuous laser activation. Risk assessment should therefore rely not only on peak and median intrarenal temperature, but also on the threshold thermal dose (CEM43 >120).

Effect of laser power on the intrarenal temperature profile.

The role of laser power as the primary determinant of the temperature profile has been convincingly demonstrated in several in vivo studies. Aldoukhi et al. [6], investigating temperature variations during Ho:YAG lithotripsy in a porcine model, demonstrated that at a

power of 40 W (0.5 J × 80 Hz), the mean time to reach the thermal injury threshold (43 °C) was 12.7 seconds (61.4 °C) in the absence of irrigation and 17.8 seconds at an irrigation rate of 15 mL/min (50.1 °C). Histological examination demonstrated that in models where laser activation was performed without irrigation, diffuse renal tissue injury was observed to a depth of 3 mm over a length of approximately 14 mm. At 15 mL/min, the depth of injury decreased to <1 mm, whereas at an irrigation rate of 40 mL/min neither critical temperature nor histological evidence of urothelial injury was observed [6].

Similar findings were reported by Marom et al. [7], who used the threshold thermal dose (CEM43 >120) to assess the safety of laser lithotripsy. The authors demonstrated that at a laser power of 48 W and an irrigation rate of 15 mL/min, CEM43 >120 was exceeded within 8–12 seconds, whereas at 25 W with the same irrigation rate this threshold was either not reached or was reached only after more than one minute of continuous activation [7].

Additional confirmation of thermal injury mechanisms was provided in a bench-top study by Ventimiglia et al. [8], in which heat distribution generated by laser radiation was analyzed in an experimental renal calyx model using thermal imaging. An increase in laser power was shown to correlate with higher maximum recorded temperatures and increased absorbed thermal dose (CEM43 >120) [8].

The findings of the present study are consistent with these observations. Increasing laser power from 25 to 35 W in our experiment resulted in an increase in median intrarenal temperature of approximately 9–10 °C for both Ho:YAG and TFL. Importantly, not only absolute temperature elevation but also a marked reduction in the time required to reach subcritical and critical temperature thresholds was observed. At an irrigation rate of 15 mL/min, 43 °C during Ho:YAG activation was reached in 19 seconds at 25 W and in 5 seconds at 35 W, whereas during TFL activation 43 °C was reached in 26 and 9 seconds, respectively. Thus, increasing laser power by 10 W reduced the time to reach the 43 °C threshold by 14

seconds for Ho:YAG and by 17 seconds for TFL. CEM43 values greater than 120 were observed at the maximum power setting of 35 W in combination with the minimum irrigation rate of 15 mL/min for both laser systems. In summary, increasing laser power elevates intrarenal temperature while simultaneously shortening the duration of safe lithotripsy.

Effect of irrigation as a key modifiable factor of thermal safety.

The protective role of irrigation has been consistently confirmed in both experimental and clinical studies. Dau et al. [9] demonstrated, in a simulation of Ho:YAG laser lithotripsy in an animal model, that increasing the irrigation rate and using a chilled solution at fixed laser power resulted in a reduction of the maximum intrarenal temperature by 5–8 °C and more than a twofold increase in the time required to reach the 43 °C threshold. Specifically, at an irrigation rate of 8 mL/min, 43 °C was reached regardless of the temperature of the irrigation solution, whereas the use of a chilled solution at 12 mL/min or a room-temperature solution at 15 mL/min resulted in the 43 °C threshold not being reached throughout the entire experiment [9].

Clinical data also confirm the interrelation between intrarenal temperature and irrigation parameters. In a prospective clinical study, Kose et al. [10] estimated the intrarenal temperature dynamics in patients undergoing retrograde intrarenal surgery for urolithiasis using a Ho:YAG laser. A key feature of this study was its clinical design, as temperature measurements were performed directly during surgery without experimental simulation and with preservation of all factors inherent to real clinical practice, including physiological renal perfusion, fluctuations in intrarenal pressure, and variability in irrigation outflow. A miniature thermosensor integrated into the working channel of the ureteroscope was used for temperature recording, enabling continuous real-time monitoring of intrarenal temperature within the renal collecting system. The study showed that increasing the irrigation rate from

10 to 20 mL/min was associated with a decrease in mean intrarenal temperature of nearly 5 °C and a reduction in the frequency of episodes exceeding the 43 °C threshold [10].

In our study, similar patterns were observed; however, the effect of increasing the irrigation rate was more pronounced. Increasing the irrigation rate from 15 to 20 mL/min resulted in a reduction in median intrarenal temperature of 4–5 °C for both Ho:YAG and TFL, as well as a decrease in the time to and likelihood of reaching critical peak temperatures and exceeding the threshold thermal dose CEM43 >120.

Effect of laser type: Ho:YAG and TFL in the context of thermal risk.

Comparison of the thermal effects of holmium and thulium fiber lasers remains an area of active investigation.

Okhunov et al. [11], in an in vivo porcine model, demonstrated that in all experimental series using TFL in dusting mode (0.5 J × 80 Hz – 40 W) and fragmentation modes (1 J × 10 Hz – 10 W and 1.5 J × 20 Hz – 30 W), absence of irrigation outflow was associated with an increase in intrarenal temperature within the calyx above 44 °C, regardless of irrigation fluid temperature (20–22 °C or 37 °C) [11].

In a prospective study, Gupta et al. [12] evaluated intrarenal temperature dynamics during endoscopic combined intrarenal surgery (ECIRS). Temperature monitoring was performed in 20 patients (10 in the Ho:YAG group and 10 in the TFL group) during the procedure using invasive thermocouples placed in the renal parenchyma. The authors measured intrarenal and parenchymal temperatures in fragmentation modes (1 J/2 Hz TFL and 0.5 J/5 Hz Ho:YAG, 2–2.5 W), dusting (0.3 J/50 Hz, 15 W), and pop-dusting (0.5 J/80 Hz, 40 W) for 2 minutes. In dusting mode, the maximum intrarenal temperature within the calyces reached 51 °C and 56 °C with TFL and Ho:YAG, respectively. Parenchymal temperature exceeded 43 °C in one patient (Ho:YAG group), reaching 49 °C at 60 seconds. The mean maximum temperature in

pop-dusting mode was higher with TFL (52.9 °C vs 45.1 °C). Maximum parenchymal temperatures were 47 °C and 49 °C, respectively [12].

Complementing the in vivo data, Æsøy et al. [13] performed a direct comparison of temperature profiles in an experimental ex vivo porcine kidney model using Ho:YAG and TFL, with recording of intrarenal temperature in both the renal collecting system and renal parenchyma [13]. The authors demonstrated that increasing laser power was accompanied by a proportional rise in temperature: with a 150 µm fiber, increasing power from 2.4 to 20 W resulted in an average intrarenal temperature increase from 2.6 to 19.9 °C relative to baseline. At identical power settings, increasing fiber diameter was associated with greater heating (at 20 W, mean temperature was 39.6 °C for a 150 µm fiber and 44.9 °C for a 200 µm fiber). The 43 °C threshold was exceeded at powers of 20–30 W after 18–44 seconds of continuous activation under gravitational irrigation (~60 cm H_2O), whereas at lower power settings (2.4–8 W) this threshold was not reached. At 20 W, peak intrarenal temperatures in the pelvis were 52.1 °C for TFL and 51.3 °C for Ho:YAG, with corresponding parenchymal temperatures of 26.8 °C and 27.5 °C. At 30 W, peak intrarenal temperatures in the pelvis were 60.9 °C for TFL and 61.8 °C for Ho:YAG, with parenchymal temperatures of 31.6 °C and 30.4 °C, respectively [13].

Similar to Æsøy et al. [13], the absolute differences in median intrarenal temperature between Ho and TFL were modest under all evaluated conditions, ranging from 1.88 to 2.25 °C. Taking into account the magnitude of the observed differences, the manufacturer-specified measurement accuracy of the thermocouples (±1.5 °C), and the SEM of the pointwise mean temperature profiles, the clinical relevance of these differences appears limited. Furthermore, the differences between laser systems were smaller than the temperature changes associated with increasing laser power or reducing the irrigation rate. These findings suggest that laser type was not the primary determinant of the observed

thermal profile, whereas laser power, irrigation rate, and duration of continuous activation appeared to have a greater influence.

Effect of critical temperature elevation on surrounding tissues.

The issue of thermal impact on the renal parenchyma is of fundamental importance for the clinical interpretation of thermal injury risk, since damage to the renal tissue and urothelium determines the potential functional consequences of laser lithotripsy. In an in vivo study by Bonzagni et al. [14], a direct assessment of temperature parameters and thermal dose in ureteral tissue was performed using Ho:YAG with implanted thermocouples. The authors demonstrated that exceeding the thermal damage threshold CEM43 >120 at a laser power of 20 W and an irrigation rate of less than 10 mL/min may occur within 10–30 seconds of continuous laser activation, while the peak irrigation fluid temperature in several cases did not exceed 45–47 °C [14].

Similar findings were previously reported by Aldoukhi et al. [6], who showed that during Ho:YAG lithotripsy the temperature in the collecting system could reach 63–85 °C, whereas parenchymal temperature in most measurements remained below 40–42 °C. The authors attributed this to the buffering effect of renal tissue perfusion, which provides physiological heat dissipation. At the same time, they emphasized that the relative thermal stability of the parenchyma does not exclude the formation of localized microzones of thermal injury in proximity to the collecting system [6].

The morphological findings obtained in the present study complement and confirm these observations. In our experiment, despite the fact that the median intrarenal temperature reached maximum values up to 55.27 °C, parenchymal temperature remained relatively stable and did not exceed 43 °C in any experiment, and the parenchymal CEM43 >120 threshold was likewise not exceeded. However, morphological alterations of renal tissue

observed when both laser systems were used at 35 W with an irrigation rate of 15 mL/min indicate that exceeding the threshold thermal dose (CEM43 >120) in the irrigation fluid should be regarded as a key indicator of the risk of parenchymal thermal injury, since these changes were observed under conditions where CEM43 >120 was exceeded for the irrigation medium, while the parenchymal CEM43 >120 threshold was not exceeded.

The apparent discrepancy between the relatively stable parenchymal temperature and the presence of histopathological injury may be explained by spatial differences between temperature measurement and tissue sampling. The parenchymal thermocouple was positioned at a depth of 5 mm, whereas the observed tissue injury was confined predominantly to the urothelial and suburothelial layers, with a maximum depth of 590.3 µm. Therefore, the absence of temperatures above 43 °C at the parenchymal measurement site does not exclude steep local temperature gradients or focal superficial thermal injury adjacent to the collecting system.

Histologically, the alterations were characterized by focal cellular injury without linear defects or carbonization, allowing to attribute the damage to the temperature and not the direct contact between the laser fiber and tissue. The pattern of injury indicates indirect thermal damage, most likely caused by local overheating of the fluid environment within the collecting system.

Thus, the combined literature data and our own findings suggest that the renal parenchyma indeed functions as an effective thermal buffer limiting deep heat propagation. However, this feature does not eliminate the possibility of microstructural injury occurring when the threshold thermal dose of the irrigation fluid is exceeded.

Study limitations. Despite standardized experimental conditions, this study has several limitations. The principal limitation was the exploratory sample size of 10 animals, with only

two kidneys evaluated per primary experimental condition. No formal a priori sample size calculation was performed, and the number of animals was determined by experimental feasibility and considerations related to minimizing animal use. The limited number of kidneys per condition precluded robust inferential analysis. Furthermore, serial temperature measurements obtained within the same kidney were temporally correlated and were therefore not treated as independent observations. Nevertheless, the study design yielded consistent descriptive patterns regarding the thermal effects associated with the evaluated laser systems and experimental settings.

Conclusions. In this in vivo porcine model of simulated endoscopic laser lithotripsy, intrarenal thermal profiles were influenced predominantly by laser power, irrigation rate, and the duration of continuous laser activation. Increasing laser power was accompanied by higher intrarenal temperatures, more rapid attainment of critical temperature thresholds, and a greater likelihood of exceeding CEM43 >120. Conversely, increasing the irrigation rate was associated with lower intrarenal temperatures and delayed accumulation of the critical thermal dose.

The absolute differences in median intrarenal temperature between Ho:YAG and TFL were modest compared with the temperature changes associated with laser power and irrigation rate, suggesting that laser type was not the primary determinant of the observed thermal profile under the evaluated conditions.

The 35 W/15 mL/min condition demonstrated the least favorable thermal profile, with the highest recorded temperatures, early exceedance of CEM43 >120, and reproducible histopathological injury in the examined tissue sections. In contrast, laser activation at 25 W with irrigation rates of 15–20 mL/min showed a more favorable thermal safety profile and was not associated with CEM43 >120 or identified histopathological injury in the examined

sections. Given the exploratory design and limited number of kidneys per experimental condition, these findings require validation in larger experimental studies and under clinical conditions.

List of abbreviations:

CEM43: Cumulative equivalent minutes at 43 °C

ECIRS: Endoscopic combined intrarenal surgery

Ho:YAG: Holmium:yttrium–aluminum–garnet

Q1: First quartile

Q3: Third quartile

RIRS: Retrograde intrarenal surgery

SEM: Standard error of the mean

TFL: Thulium fiber laser

Declarations

Ethics approval and consent to participate

All experimental procedures involving animals were reviewed and approved by the Interuniversity Ethics Committee (Minutes No. 07-26, dated 16 July 2026).

Consent for publication

Not applicable.

Availability of data and materials

The datasets used and/or analysed during the current study are available from the corresponding author on reasonable request.

Competing interests

The authors declare that they have no competing interests.

Funding

The study was supported by the Moscow Center for Innovative Technologies in Healthcare.

Authors' contributions

VM: Conceptualization, Methodology, Supervision, Writing – review & editing. VG: Methodology, Writing – review & editing. BS: Writing – review & editing. SS: Conceptualization, Methodology, Investigation, Data curation, Formal analysis, Visualization, Writing – original draft. IG: Methodology, Investigation, Writing – review & editing, Data curation. LR: Investigation (pathomorphological analysis), Writing – review & editing. ATa: Formal analysis, Writing – review & editing. NG: Writing – review & editing. ATs: Methodology, Writing – review & editing. DP: Supervision, Resources, Writing – review & editing.

All authors contributed to manuscript revision and read and approved the submitted version.

Acknowledgements

Not applicable.

References.

1. Gadzhiev N, Prosyannikov M, Malkhasyan V, Akopyan G, Somani B, Sivkov A, et al. Urolithiasis prevalence in the Russian Federation: analysis of trends over a 15-year period. World J Urol. 2021;39(10):3939–3944. doi:10.1007/s00345-021-03729-y.

2. Jahrreiss V, Ripa F, Somani B. Outcomes of ureteroscopy and laser fragmentation using a 60 W MOSES laser: a 3-year prospective study from a University Teaching Hospital. Ther Adv Urol. 2024;16:17562872241272033. doi:10.1177/17562872241272033.

592 3. Traxer O, Keller EX. Thulium fiber laser: the new player for kidney stone treatment? A
593 comparison with Holmium:YAG laser. World J Urol. 2020;38(8):1883–1894.
594 doi:10.1007/s00345-019-02654-5.
595 4. Sapareto SA, Dewey WC. Thermal dose determination in cancer therapy. Int J Radiat
596 Oncol Biol Phys. 1984;10(6):787–800. doi:10.1016/0360-3016(84)90379-1.
597 5. Tonyali S, von Bargen MF, Ozkan A, Gratzke C, Miernik A. The heat is on: the impact of
598 excessive temperature increments on complications of laser treatment for ureteral and
599 renal stones. World J Urol. 2023;41(12):3853–3865. doi:10.1007/s00345-023-04652-0.
600 6. Aldoukhi AH, Hall TL, Ghani KR, Maxwell AD, MacConaghy B, Roberts WW. Caliceal fluid
601 temperature during high-power holmium laser lithotripsy in an in vivo porcine model. J
602 Endourol. 2018;32(8):724–729. doi:10.1089/end.2018.0395.
603 7. Marom R, Dau JJ, Hall TL, Ghani KR, Louters MM, Kim HJ, et al. Thermal safety boundaries
604 for laser power and irrigation rate during ureteroscopy: in vivo porcine assessment with a
605 Ho:YAG laser. Urology. 2023;180:81–85. doi:10.1016/j.urology.2023.07.014.
606 8. Ventimiglia E, Robesti D, Keller EX, Corsini C, Folcia A, Fantin M, et al. Temperature
607 profile during endourological laser activation: introducing the thermal safety distance
608 concept. World J Urol. 2024;42(1):453. doi:10.1007/s00345-024-05162-3.
609 9. Dau JJ, Khajeh NR, Hall TL, Roberts WW. Chilled irrigation for control of temperature
610 elevation during ureteroscopic laser lithotripsy: in vivo porcine model. J Endourol.
611 2022;36(3):403–409. doi:10.1089/end.2021.0537.
612 10. Kose E, Bostanci Y, Gulsen M, Sahin F, Kalayci O, Ozden E, et al. Monitoring intrarenal
613 temperature changes during Ho:YAG laser lithotripsy in patients undergoing retrograde
614 intrarenal surgery: a novel pilot study. Urolithiasis. 2024;52(1):86. doi:10.1007/s00240-024-
615 01592-1.

11. Okhunov Z, Jiang P, Afyouni AS, Ayad M, Arada R, Brevik A, et al. Caveat emptor: the heat is “ON”—an in vivo evaluation of the thulium fiber laser and temperature changes in the porcine kidney during dusting and fragmentation modes. J Endourol. 2021;35(11):1716–1722. doi:10.1089/end.2021.0206.

12. Gupta K, Connors C, Savin Z, Lundon D, Khargi R, Durbhakula V, et al. Laser lithotripsy induces dose-dependent temperature elevation during retrograde intrarenal surgery. J Endourol. 2026;40(1):17–25. doi:10.1177/08927790251392232.

13. Æsøy MS, Juliebø-Jones P, Beisland C, Ulvik Ø. Temperature profiles during ureteroscopy with thulium fiber laser and holmium:YAG laser: findings from a pre-clinical study. Scand J Urol. 2022;56(4):313–319. doi:10.1080/21681805.2022.2104367.

14. Bonzagni AF, Hall TL, Marom R, Ghani KR, Roberts WW. Ureteral tissue temperature during ureteroscopy with Ho:YAG laser activation in an in vivo porcine model. Urology. 2025;200:11–17. doi:10.1016/j.urology.2025.02.043.

Figure captions:

Figure 1. Exposed porcine kidney: (1) parenchymal thermocouple; (2) intrarenal thermocouple; (3) ureteral access sheath.

Figure 2**.** Renal collecting system of the porcine kidney: (1) intrarenal thermocouple; (2) laser fiber.

Figure 3. Intrarenal temperature profiles under all experimental conditions.

Figure 4. Parenchymal temperature profiles under all experimental conditions.

Figure 5. Intrarenal temperature profiles: Ho:YAG.

Figure 6. Intrarenal temperature profiles: TFL.

Figure 7. Comparison of Ho:YAG and TFL at 25 W and 15 mL/min.

Figure 8. Comparison of Ho:YAG and TFL at 25 W and 20 mL/min.

Figure 9. Comparison of Ho:YAG and TFL at 35 W and 15 mL/min.

Figure 10. Comparison of Ho:YAG and TFL at 35 W and 20 mL/min.

Figure 11. Histopathological changes following TFL activation 35 W and 15 mL/min.

Figure 12. Gross kidney section following Ho:YAG activation 35 W and 15 mL/min.

Figure 13. Histological changes following Ho:YAG activation 35 W and 15 mL/min.

Figure 14. Control histological specimen.

Tables.

Table 1. Median intrarenal and parenchymal temperatures at different laser power settings and irrigation rates.

Laser Type	Laser power	Irrigation rate	Median intrarenal temperature	Median parenchymal temperature
Ho:YAG	25 W	15 ml/min	45.25 (44.84; 45.62) °C	37.13 (37; 37.375) °C
Ho:YAG	25 W	20 ml/min	41.50 (41.12; 41.75) °C	36.75 (36.5; 36.875) °C
Ho:YAG	35 W	15 ml/min	55.27 (53.65; 55.75) °C	39.33 (38.875; 39.625) °C
Ho:YAG	35 W	20 ml/min	50.25 (48.1; 50.62) °C	38 (37.5; 38.325) °C
TFL	25 W	15 ml/min	43.37 (43; 43.5) °C	37.75 (37.5; 37.875) °C
TFL	25 W	20 ml/min	39.25 (39.12; 39.62) °C	37.56 (37.47; 37.75) °C
TFL	35 W	15 ml/min	53.12 (49.68; 53.37) °C	38.50 (38; 38.75) °C
TFL	35 W	20 ml/min	48.00 (46.56; 48.5) °C	37.25 (37.125; 37.375) °C

Notes: Temperatures were recorded during 120 seconds of continuous laser activation. At each time point, temperature values obtained from two kidneys were averaged, generating a 120-point mean temperature profile for each experimental condition. Data are presented as median [Q1; Q3] calculated from the corresponding mean temperature profile.

Table 2. Peak intrarenal and parenchymal temperatures at different laser power settings and irrigation rates.

Laser Type	Laser power	Irrigation rate	Peak intrarenal temperature	Peak parenchymal temperature
Ho:YAG	25 W	15 ml/min	45.75 °C	37.38 °C
Ho:YAG	25 W	20 ml/min	42.75 °C	36.63 °C
Ho:YAG	35 W	15 ml/min	56.13 °C	40.38 °C
Ho:YAG	35 W	20 ml/min	50.88 °C	38.75 °C
TFL	25 W	15 ml/min	43.63 °C	38.00 °C

TFL	25 W	20 ml/min	39.88 °C	37.88 °C
TFL	35 W	15 ml/min	53.86 °C	38.88 °C
TFL	35 W	20 ml/min	48.86 °C	37.63 °C

Notes: Temperatures were recorded during 120 seconds of continuous laser activation. Peak temperatures represent the maximum values recorded in the 120-point mean temperature profile generated from two kidneys for each experimental condition.

Table 3. Time to reach intrarenal temperature thresholds of 43 and 56 °C.

Ho:YAG		
Condition	Time to 43 °C (s)	Time to 56 °C (s)
25 W 15 mL/min	19	Not reached
25 W 20 mL/min	Not reached	Not reached
35 W 15 mL/min	5	60
35 W 20 mL/min	13	Not reached
TFL		
25 W 15 mL/min	26	Not reached
25 W 20 mL/min	Not reached	Not reached
35 W 15 mL/min	9	Not reached
35 W 20 mL/min	16	Not reached

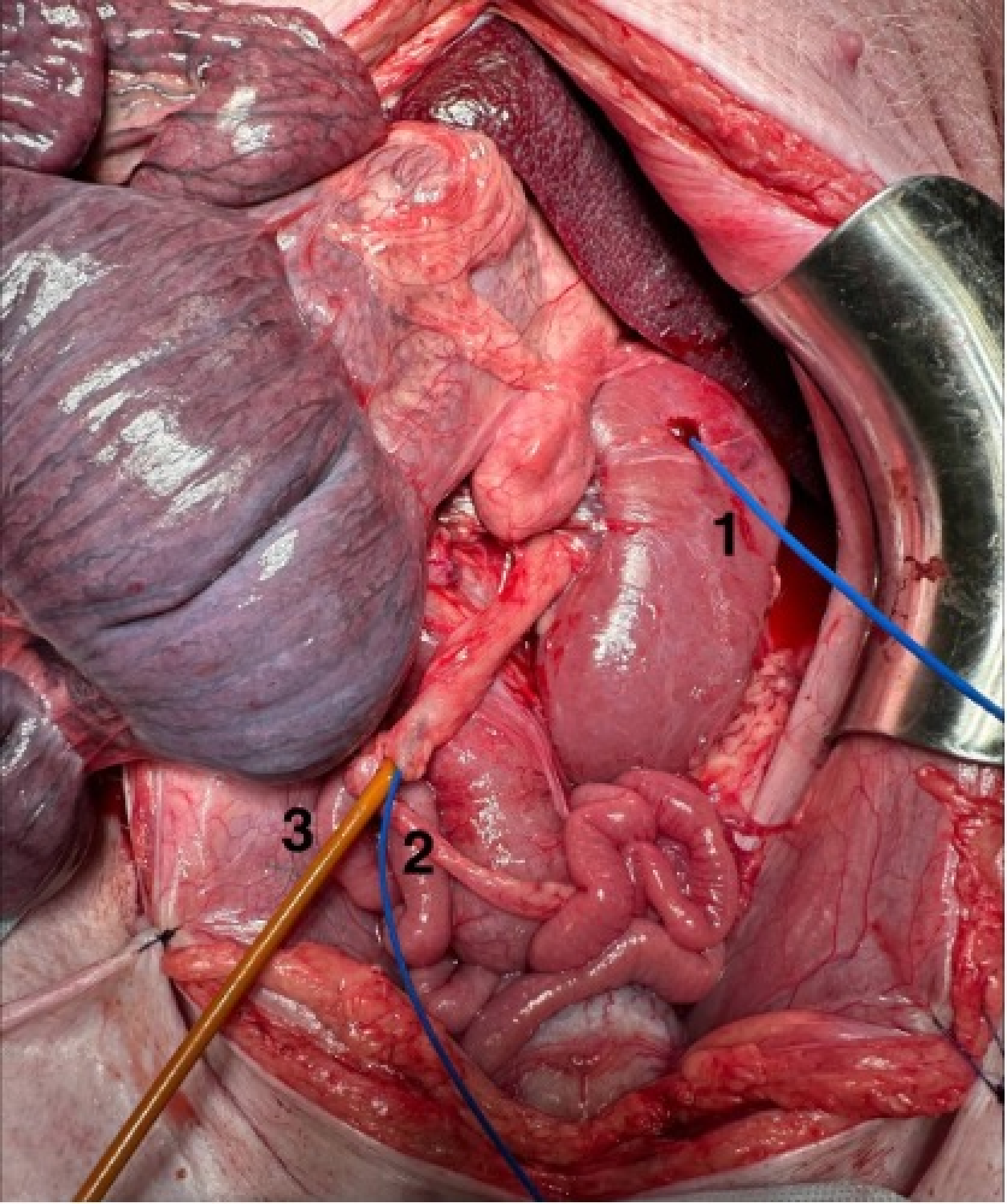
Notes: Threshold times were determined from the 120-point mean temperature profile generated from two kidneys for each experimental condition. “Not reached” indicates that the respective threshold was not achieved during the 120-second activation period.

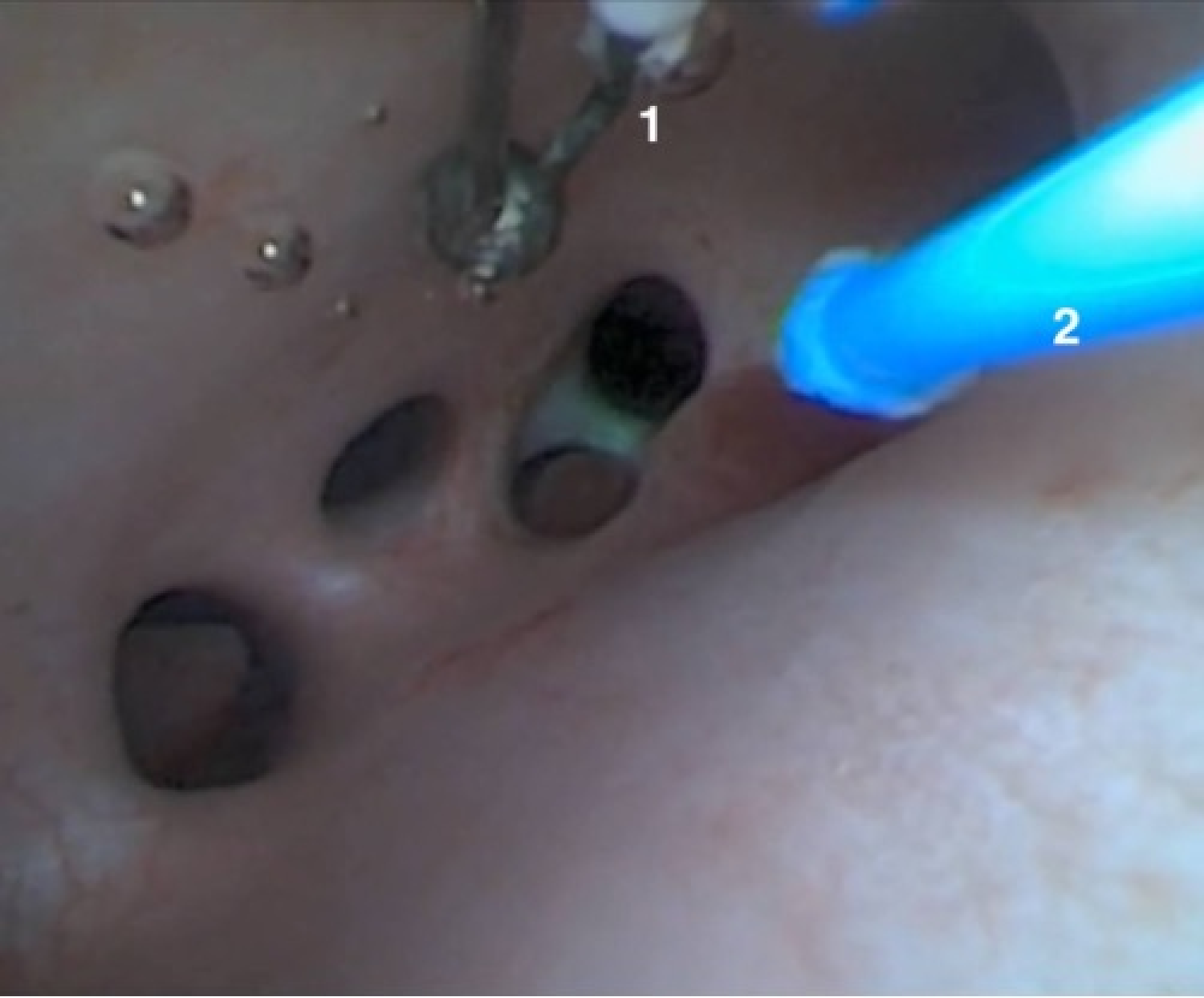
Table 4. Histopathological findings under different laser exposure settings.

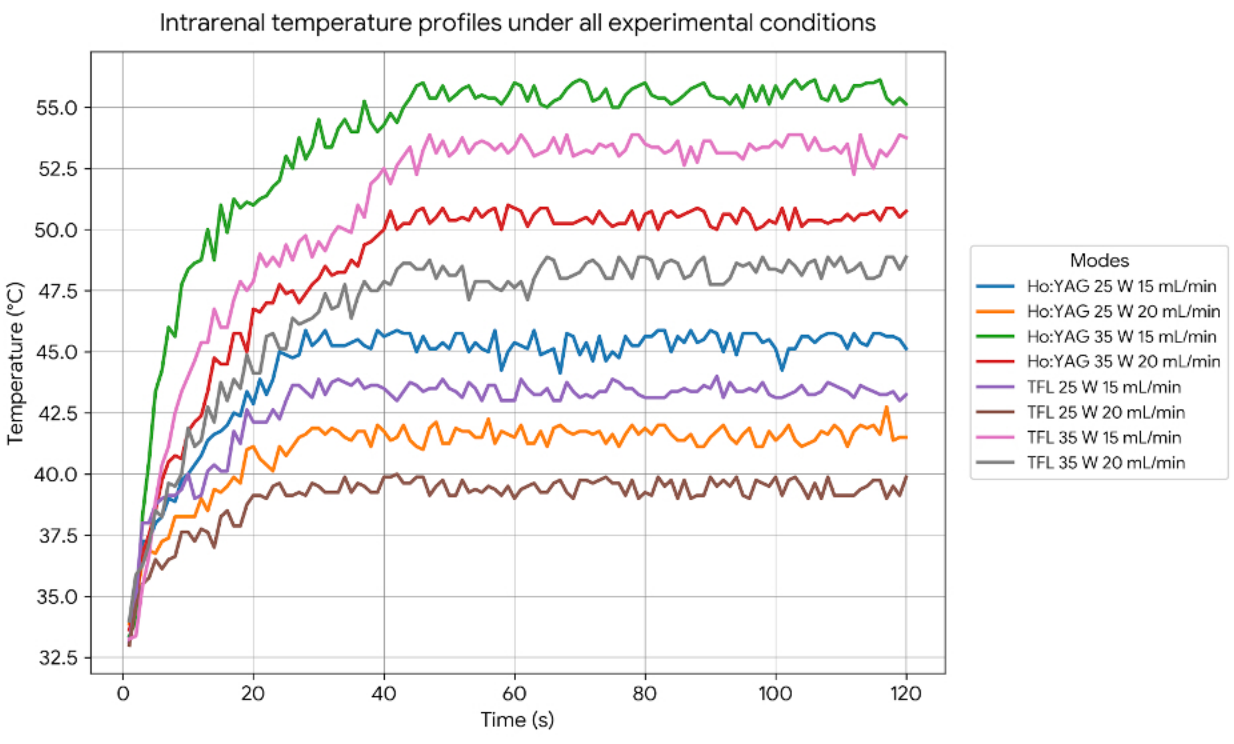
Laser type	Condition	Macroscopic damage	Mucosal layer	Depth of injury (μm)
TFL	25 W 15 ml/min	No	Preserved	-
TFL	25 W 20 ml/min	No	Preserved	-
TFL	35 W 15 ml/min	Yes	Absent	332.4 - 410.4
TFL	35 W 20 ml/min	No	Preserved	-
Ho:YAG	25 W 15 ml/min	No	Preserved	-
Ho:YAG	25 W 20 ml/min	No	Preserved	-
Ho:YAG	35 W 15 ml/min	Yes	Absent	485.1 - 590.3
Ho:YAG	35 W 20 ml/min	No	Preserved	-

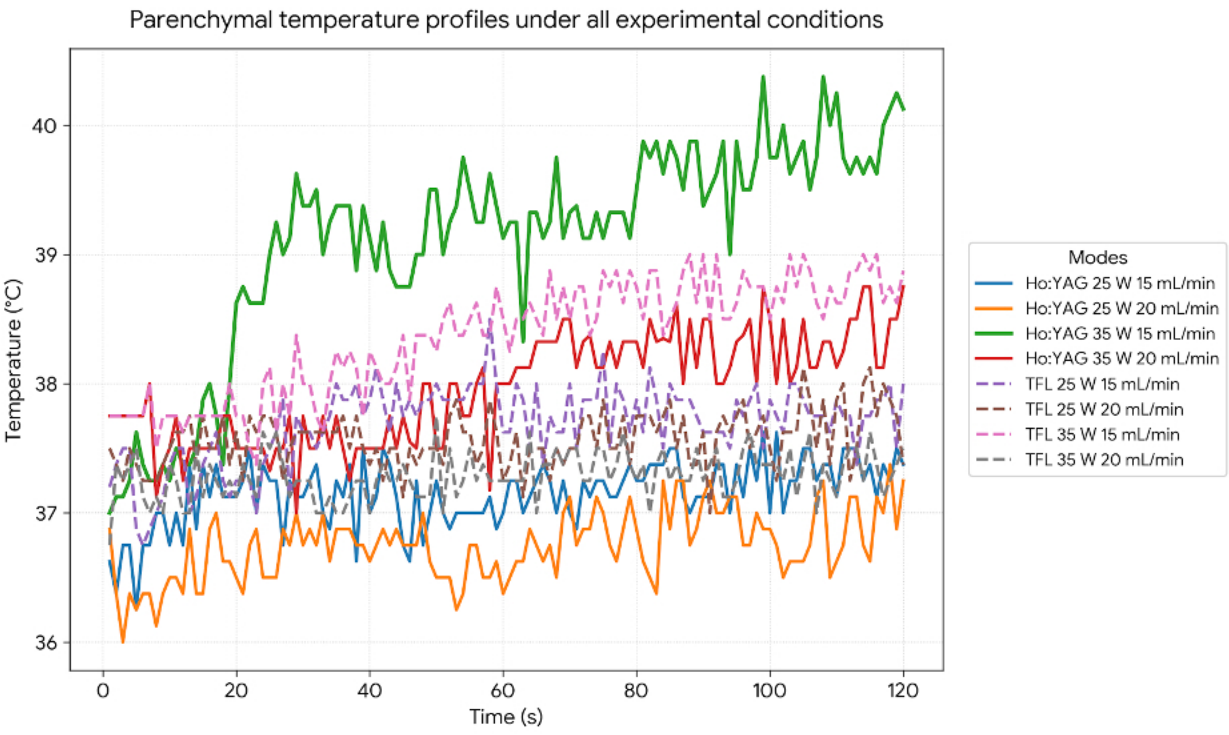
678 Notes: Two kidneys were evaluated per primary experimental condition. Injury depth is

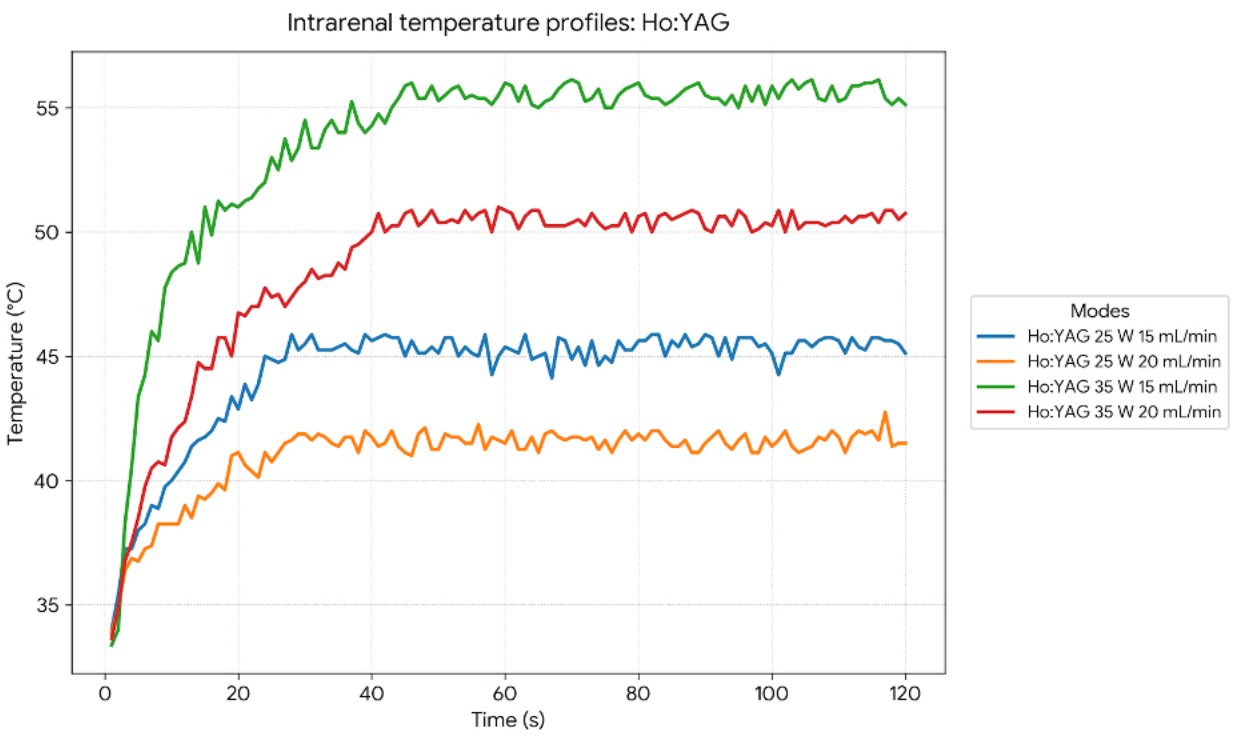
679 presented as the range of values measured in the two examined specimens.

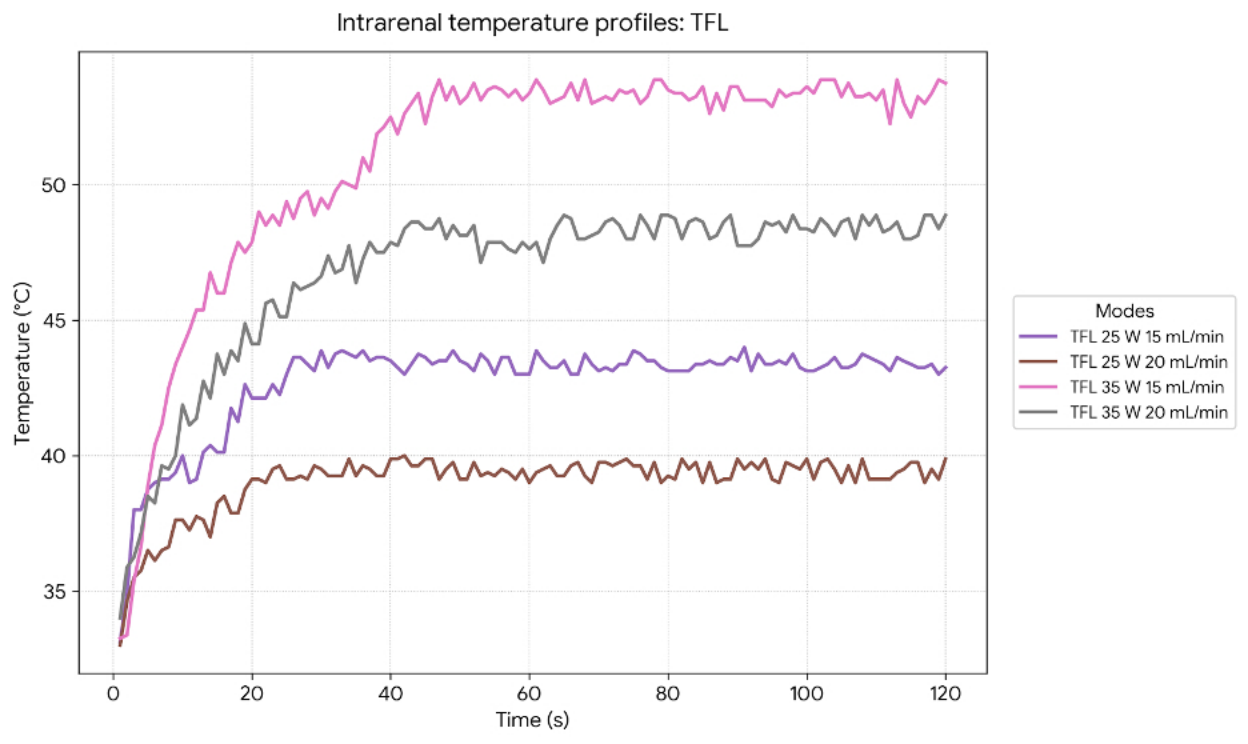

1
2
3

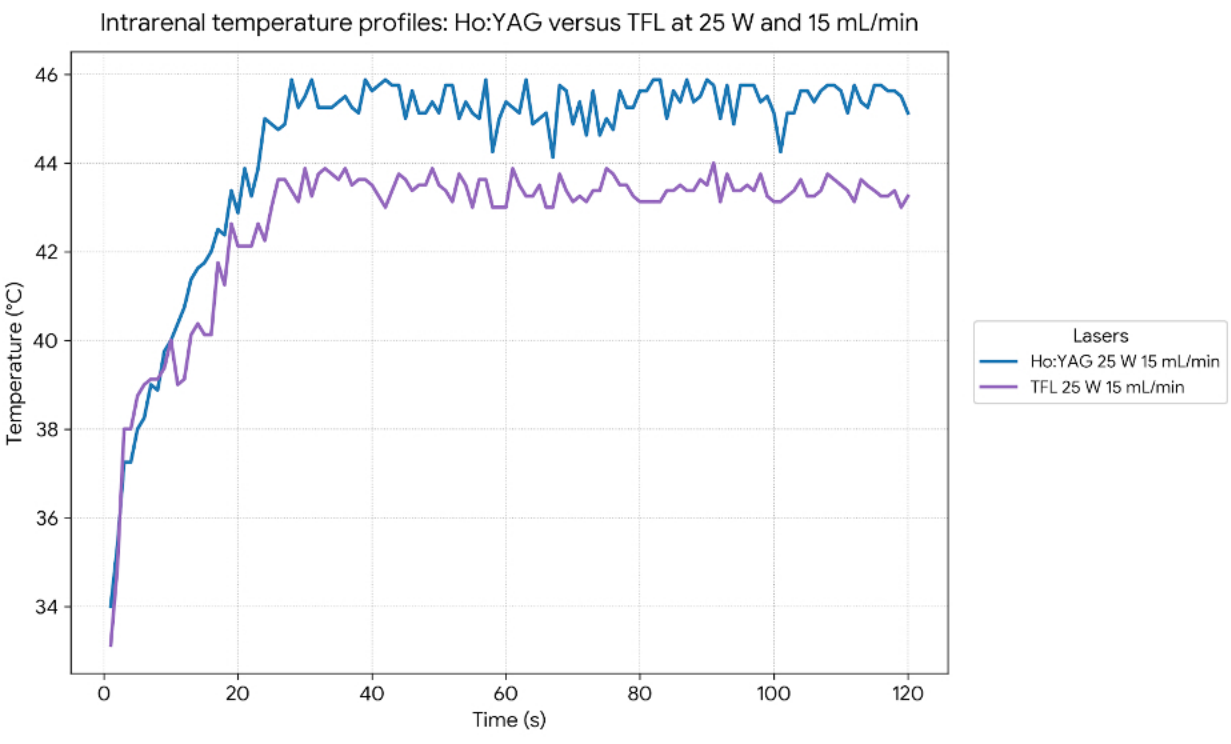

1
2

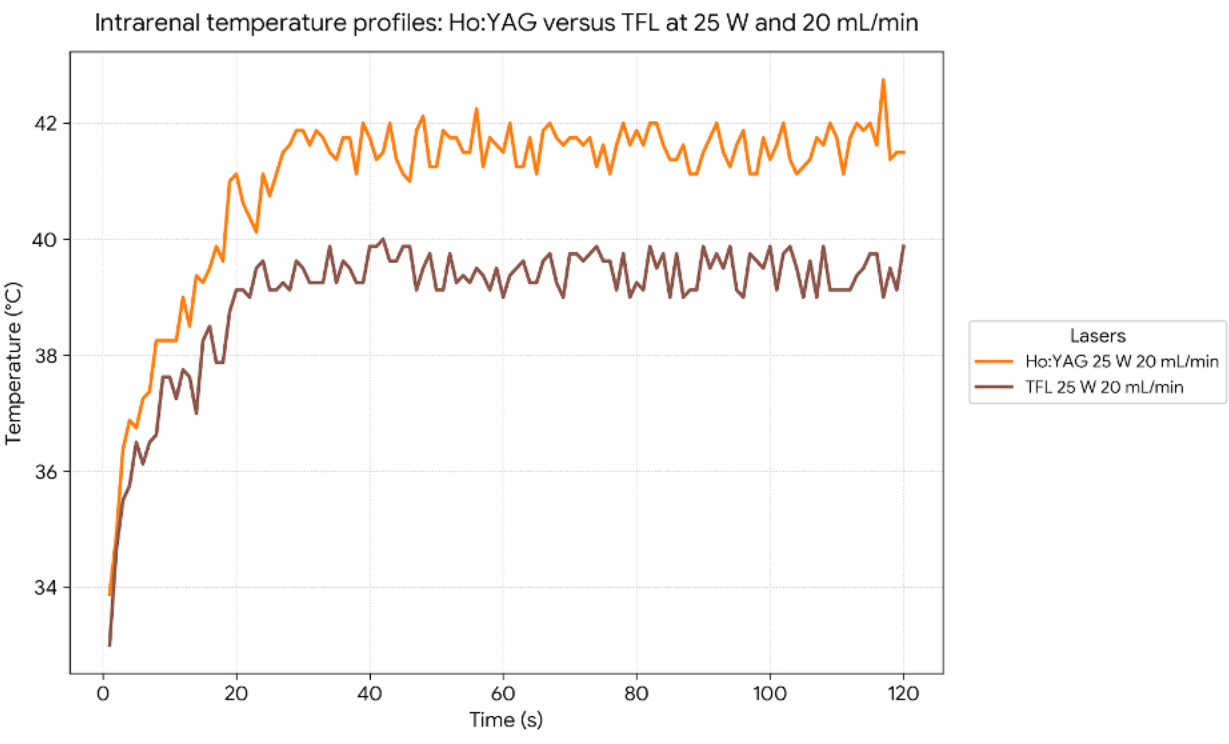

Intrarenal temperature profiles under all experimental conditions
Temperature (°C)
55.0
52.5
50.0
47.5
45.0
42.5
40.0
37.5
35.0
32.5
0
20
40
60
80
100
120
Time (s)
Modes
Ho:YAG 25 W 15 mL/min
Ho:YAG 25 W 20 mL/min
Ho:YAG 35 W 15 mL/min
Ho:YAG 35 W 20 mL/min
TFL 25 W 15 mL/min
TFL 25 W 20 mL/min
TFL 35 W 15 mL/min
TFL 35 W 20 mL/min

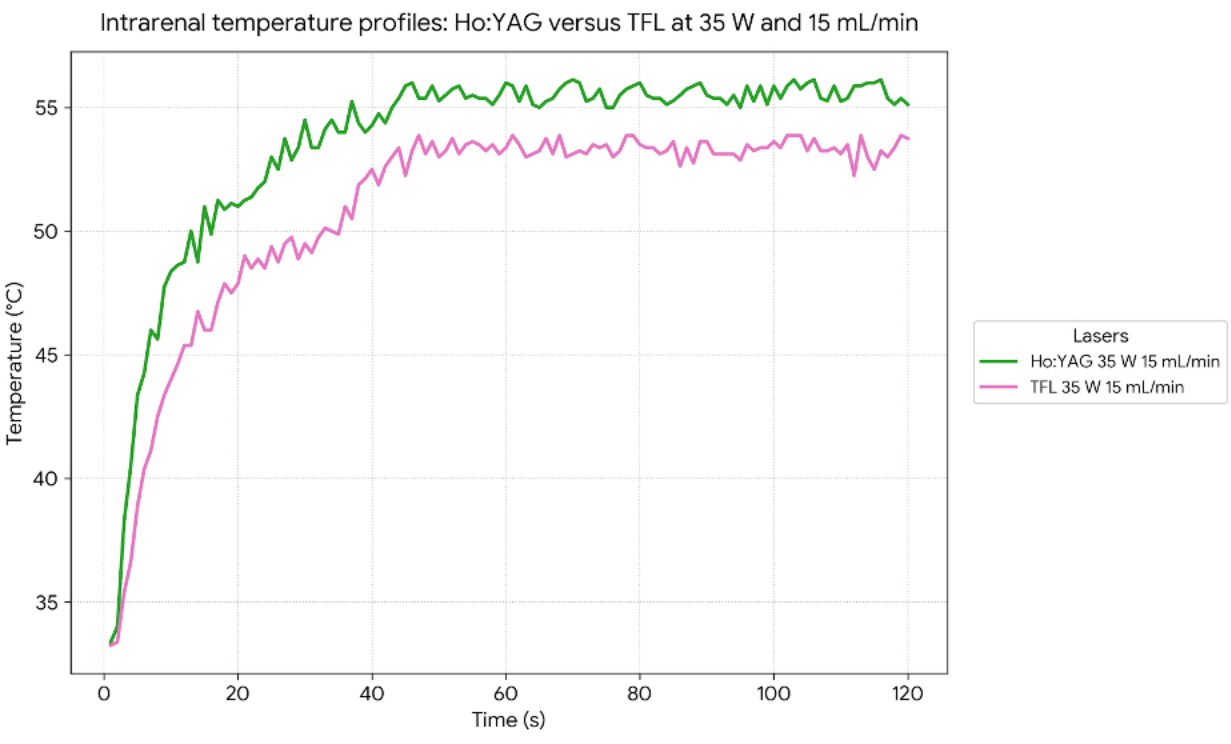

Parenchymal temperature profiles under all experimental conditions
Temperature (°C)
Time (s)
36
37
38
39
40
0
20
40
60
80
100
120
Modes
Ho:YAG 25 W 15 mL/min
Ho:YAG 25 W 20 mL/min
Ho:YAG 35 W 15 mL/min
Ho:YAG 35 W 20 mL/min
TFL 25 W 15 mL/min
TFL 25 W 20 mL/min
TFL 35 W 15 mL/min
TFL 35 W 20 mL/min

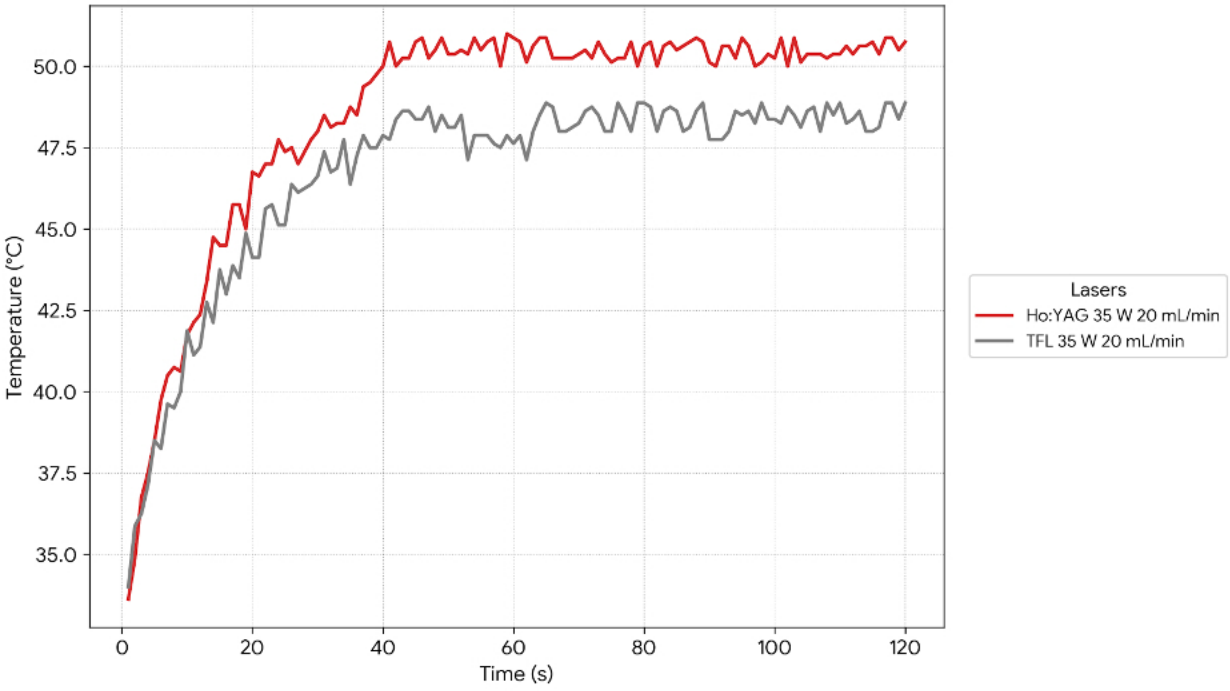

Intrarenal temperature profiles: Ho:YAG
Temperature (°C)
55
50
45
40
35
0
20
40
60
80
100
120
Time (s)
Modes
Ho:YAG 25 W 15 mL/min
Ho:YAG 25 W 20 mL/min
Ho:YAG 35 W 15 mL/min
Ho:YAG 35 W 20 mL/min

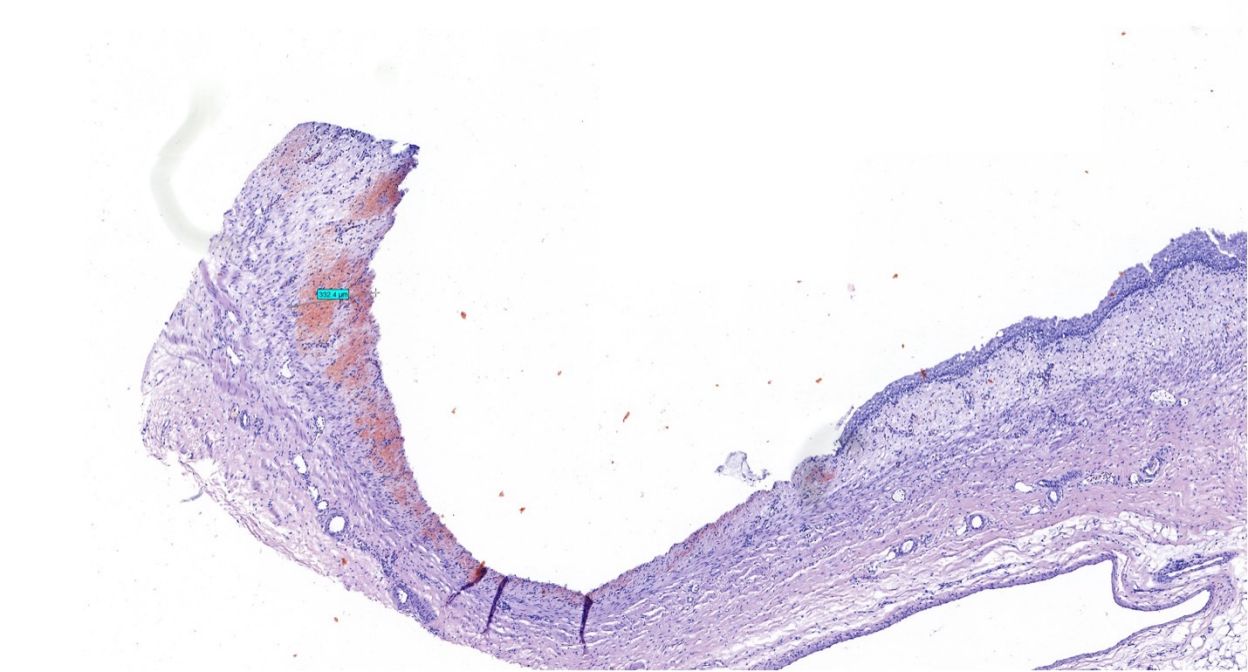

Intrarenal temperature profiles: TFL
Temperature (°C)
35
40
45
50
0
20
40
60
80
100
120
Time (s)
Modes
TFL 25 W 15 mL/min
TFL 25 W 20 mL/min
TFL 35 W 15 mL/min
TFL 35 W 20 mL/min


Intrarenal temperature profiles: Ho:YAG versus TFL at 25 W and 15 mL/min
Temperature (°C)
46
44
42
40
38
36
34
0
20
40
60
80
100
120
Time (s)
Lasers
Ho:YAG 25 W 15 mL/min
TFL 25 W 15 mL/min

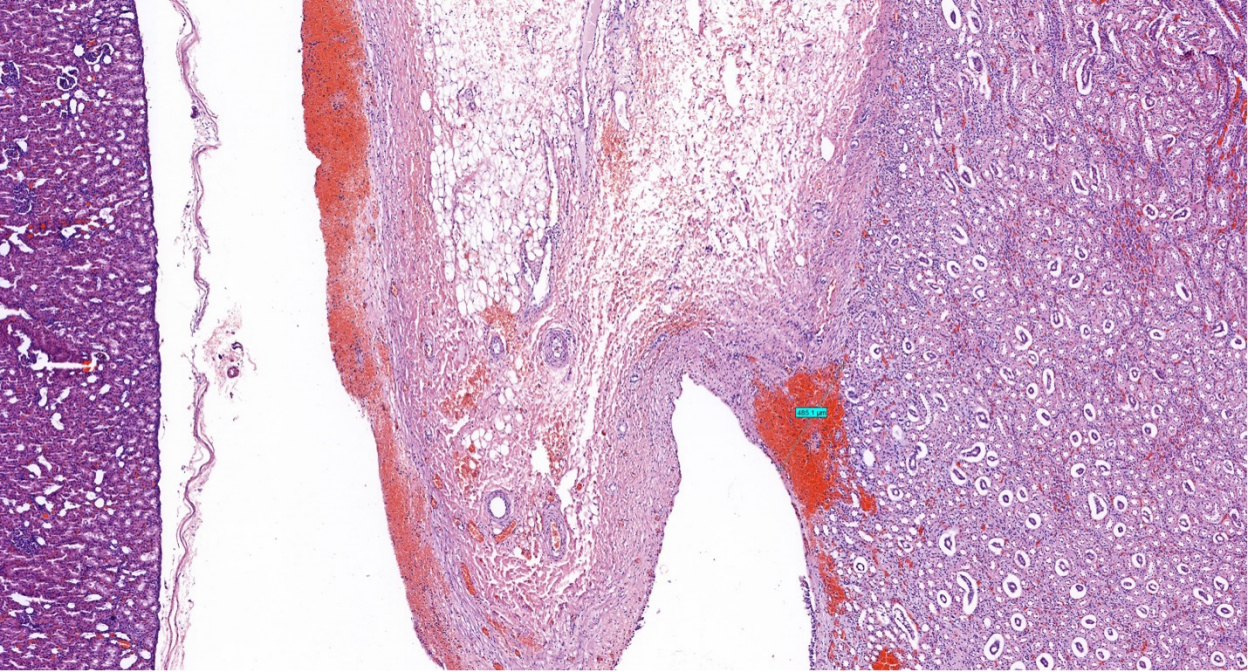

Intrarenal temperature profiles: Ho:YAG versus TFL at 25 W and 20 mL/min
Temperature (°C)
42
40
38
36
34
0
20
40
60
80
100
120
Time (s)
Lasers
Ho:YAG 25 W 20 mL/min
TFL 25 W 20 mL/min


Intrarenal temperature profiles: Ho:YAG versus TFL at 35 W and 15 mL/min
Temperature (°C)
55
50
45
40
35
0
20
40
60
80
100
120
Time (s)
Lasers
Ho:YAG 35 W 15 mL/min
TFL 35 W 15 mL/min


Intrarenal temperature profiles: Ho:YAG versus TFL at 35 W and 20 mL/min
Temperature (°C)
50.0
47.5
45.0
42.5
40.0
37.5
35.0
0
20
40
60
80
100
120
Time (s)
Lasers
Ho:YAG 35 W 20 mL/min
TFL 35 W 20 mL/min


532.4 µm


25


485.1 µm

